Journal of Organometallic Chemistry 1022 (2024) 123385

Contents lists available at ScienceDirect

Journal of Organometallic Chemistry

journal homepage: www.elsevier.com/locate/jorganchem

Protective effect of the perchlorophenyl group in organophosphorus chemistry☆

Mª Ángeles García-Monforte, Miguel Baya, Antonio Martín, Babil Menjón *

Instituto de Síntesis Química y Catálisis Homogénea (iSQCH), CSIC–Universidad de Zaragoza, C/Pedro Cerbuna, 12, ES-50009, Zaragoza, Spain

ARTICLE INFO

Keywords:
Lewis acidity
Perchlorophenyl
Phosphorus
Stereochemistry
Steric shielding
Superacid

ABSTRACT

The homoleptic phosphine with the bulky perchlorophenyl group, $(C_6Cl_5)_3P$ (**1**), exhibits trigonal pyramidal structure (*TPY*-3), yet considerably flattened: Σ(C–P–C') = 321.0(1)°. Key steric and electronic properties of this simple organophosphorus species have been estimated by calculation. Attending to its characteristic features, **1** can be rated as a deactivated phosphine, where the less-basic P atom is sterically shielded by the bulky C_6Cl_5 groups. This marked inertness notwithstanding, it has been possible to obtain (under harsh conditions) derivatives with phosphorus in high oxidation state, namely the phosphine oxide $(C_6Cl_5)_3PO$ (**2**) and the difluorophosphorane $(C_6Cl_5)_3PF_2$ (**3**). These four- and five-substituted derivatives respectively exhibit trigonal pyramidal (*TPY*-4) and trigonal bipyramidal (*TBPY*-5) structures. The Σ(C–P–C') value steadily increases along the series **1**–**3**, according to the referred structural variation. The P–C bond length is, in turn, invariably maintained at about 185 pm regardless of the different oxidation state, the increasing number of substituents around the P atom and the overall geometry. The hypervalent difluorophosphorane $(C_6Cl_5)_3PF_2$ (**3**) dissociates one of the axial fluorides in the gas phase giving rise to the fluorophosphonium cation $[(C_6Cl_5)_3PF]^+$, as detected by mass spectrometry. This cation is identified as a Lewis superacid.

1. Introduction

Triarylphosphines count among the most popular tertiary phosphines used in synthetic, coordination and organometallic chemistry [1]. In general, triarylphosphines are much less air-sensitive than their alkyl counterparts and therefore much easier to handle. It is worth noting that, the archetypal representative, Ph_3P, which was prepared as early as 1882 [2], has today the greatest industrial importance of all the tertiary phosphines [3]. One of the principal reasons for the widespread use of triarylphosphines is the variability of the overall steric and electronic properties, which can be deliberately modulated by the judicious choice of the substituents at the aryl groups. New variations with ever more elaborate substituents are continuously being produced in order to achieve the desired properties. The effect of a given R group is best appreciated in homoleptic (symmetric) R_3P phosphines, where R is the sole responsible of the overall properties [4]. As it has already been noted [5], double substitution at the *ortho* positions (2,6-disubstitution) is of particular importance, as it produces the greatest steric impact on the P centre in addition to the corresponding electronic effect. Alkyl substituents such as Me and ^{i}Pr have electron-donor character, but clearly different steric requirements as evidenced in the following groups (Scheme 1): 2,6-$Me_2C_6H_3$ [6], 2,4,6-$Me_3C_6H_2$ (Mes) [7], and the very bulky 2,6-$^i Pr_2C_6H_3$ (Diip) [8] or 2,4,6-$^i Pr_3C_6H_2$ (Tiip) [9], as well as some derivatives thereof at the *para* position [10–12]. The C_6F_5 group has, in turn, a marked electron-withdrawing character with rather modest steric requirement [13]. The homoleptic phosphine with the fused-ring anthracen-9-yl is also known [14].

In the library of available aryls, the C_6Cl_5 group occupies a singular place: its electron-withdrawing character is comparable to that assigned to C_6F_5 [15], but its steric bulk is closer to that of Mes, since Cl and Me substituents are assigned similar volumes [16]. Owing to this characteristic combination of electronic and steric properties, the C_6Cl_5 group has been widely used in transition-metal chemistry [17]. A systematic study of the impact of the C_6Cl_5 group in organoboranes led to the conclusion that C_6Cl_5 is more electron-withdrawing than C_6F_5 [18]. It was demonstrated that the strong Lewis acid $(C_6Cl_5)_3B$ still forms complexes with small anions despite the steric hindrance [19]. The homologous series of triarylphosphines $(C_6Cl_5)_nPh_{3-n}P$ (n = 0–3) has

☆ Dedicated to Dr. Milagros Tomás on the occasion of her 70th birthday.

* Corresponding author at: Instituto de Síntesis Química y Catálisis Homogénea (iSQCH), CSIC–Universidad de Zaragoza, C/Pedro Cerbuna, 12, ES-50009 Zaragoza, Spain.

E-mail address: menjon@unizar.es (B. Menjón).

https://doi.org/10.1016/j.jorganchem.2024.123385
Received 15 July 2024; Received in revised form 9 September 2024; Accepted 14 September 2024
Available online 23 September 2024

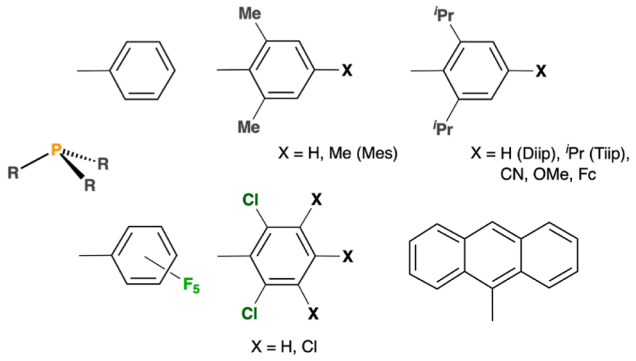

Scheme 1. Homoleptic triarylphosphines, R_3P, with a selection of representative 2,6-disubstituted aryl groups with different electronic and steric properties.

also been reported [20]. The properties ascribed to the homoleptic perchlorophenyl phosphine $(C_6Cl_5)_3P$ are, however, inconsistent with previous reports [21,22]. Its purported chemical lability is also intriguing. Aside from these conflicting reports, little is known of the homoleptic perchlorophenyl phosphine $(C_6Cl_5)_3P$. In fact, and to the best of our knowledge, no structural information is currently available and no derivative thereof has been prepared to date.

From our point of view, the molecular structure of the perchlorophenyl phosphine $(C_6Cl_5)_3P$ has particular interest, considering that the heavier homologue $(C_6Cl_5)_3Sb$ is pyramidal [23], whereas the lighter homologue $(C_6Cl_5)_3N$ is trigonal planar [24]. It is worth noting that the triad of neutral isoleptic compounds of the first-row elements, $(C_6Cl_5)_3B$ [18], $(C_6Cl_5)_3C^{\bullet}$ [25], and $(C_6Cl_5)_3N$ [24], all have similar trigonal-planar structures. In turn, the structures of the second-row analogues $(C_6Cl_5)_3Al$, $(C_6Cl_5)_3Si^{\bullet}$ and $(C_6Cl_5)_3P$ remain unknown.

In the present work, we report on the synthesis and structural characterization of the perchlorophenyl phosphine $(C_6Cl_5)_3P$ (**1**), its oxide $(C_6Cl_5)_3PO$ (**2**), and the corresponding difluorophosphorane $(C_6Cl_5)_3PF_2$ (**3**). The most fundamental properties of these chemical species are also identified and probed by theoretical methods.

2. Results and discussion

2.1. The perchlorophenyl phosphine $(C_6Cl_5)_3P$ (1)

Tris(perchlorophenyl)phosphine, $(C_6Cl_5)_3P$ (**1**), was prepared by arylation of PCl_3 with the corresponding organolithium reagent LiC_6Cl_5 in Et_2O at −78 °C (Scheme 2). The procedure is similar to that used to prepare the heavier homologue $(C_6Cl_5)_3Sb$ [23,26].

The reaction outcome would not be expected to greatly differ from that obtained in the recently reported procedure using PBr_3 as the starting material [20]. It must be noted, however, that in our own experience, the more C_6Cl_5 groups are introduced in a neutral derivative, the lower becomes its solubility. Being aware of this limitation, we preferred to free the desired product from the accompanying inorganic salts (LiCl) washing the raw residue with MeOH [27]. By so doing, a

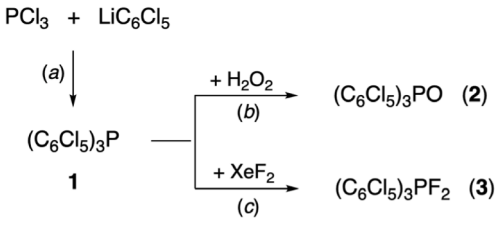

Scheme 2. Synthetic procedures leading to the perchlorophenyl phosphine **1**, its oxide **2** and the fluorophosphorane **3** under the following conditions: a) in Et_2O at low temperature starting at −78 °C; b) in boiling toluene; c) direct reaction at 110 °C with no solvent.

sparingly soluble, white solid was obtained, which was identified as the perchlorophenyl phosphine **1** by elemental analysis and spectroscopic techniques. Moreover, despite the low solubility of **1** in most organic solvents, we managed to obtain single crystals for X-ray diffraction analysis by slowly cooling down a saturated solution of **1** in CCl_4 from 80 °C to room temperature (see Experimental). In the IR spectrum, no signals corresponding to C_6Cl_5H were detected. The strong absorption at 865 cm^{-1} was assigned to the so-called X-sensitive vibration mode of the C_6Cl_5 group [28]. In the ^{31}P NMR spectrum, compound **1** shows a singlet at δ_P 9.6 ppm [in $(CH_2Cl)_2/CD_2Cl_2$ solution]. The observed chemical shift is in keeping with that originally given by Miller (δ_P 9.2 ppm; no solvent given in the original paper) [22], but largely departs from a recently reported value (δ_P 19.1 ppm in C_6D_6 solution) [20].

The structure of **1**, as obtained by single-crystal X-ray diffraction (sc-XRD) methods is shown in Fig. 1. Interatomic distances and angles are given in Table 1 [29]. In contrast to the planar geometry of the lighter homologue $(C_6Cl_5)_3N$ [24], the geometry of **1** is still pyramidal (*TPY*-3) with the typical propeller-like arrangement of the C_6Cl_5 rings around the P atom usually found in triarylphosphines as well as in the heavier homologue $(C_6Cl_5)_3Sb$ [23]. The helical arrangement of the C_6Cl_5 groups makes the molecule chiral because of the two possible orientations of the rings, clockwise (*C*) and anticlockwise (*A*), both of which are present in the centrosymmetric crystal. The structure of **1** is far from an ideal picture where the phenyl rings might be considered as rigid rotors around the P atom with overall C_3 symmetry. The actual geometry is very distorted. The angles used to describe the various sources of distortion are indicated in Fig. 2. The P atom is located 68.7(1) pm above the plane defined by the three C^{ipso} atoms. We will take the axial direction (i.e., that of the P lone pair) as defined by the P atom and the centroid of the three C^{ipso} atoms (Fig. 2a). The C_6Cl_5 rings will be numbered consecutively. The tilt of the C_6Cl_5 rings, measured by the φ angle (Fig. 2a), is unequal: two of them are tilted by ca. 50°, whereas in the remaining one, the tilt angle is as low as 16.0(1)°. Appreciably different P–C^{ipso}–C^{o} angles are also observed within the same ring depending on whether the *exo* (α) or *endo* (β) branches are considered, the largest difference being 112.4(2)° vs. 130.5(2)° in ring 3. This swing of the C_6Cl_5 rings brings each *exo*-Cl^{o} substituent closer to the P center (P···Cl ca. 300 pm) than the corresponding *endo*-Cl^{o} substituent (P···Cl ca. 350 pm). Finally, the C_6Cl_5 rings are also clearly skewed from their respective P–C bond lines (τ angle in Fig. 2b), showing deviations between 7° and 10° (Table 1).

As we see, the geometric parameters of **1** show evidence of significant steric crowding. The heavy distortions found in the stereochemistry of phosphines with crowded aryl groups were carefully analyzed by Boeré and Zhang [5]. As suggested by these authors, we will also take

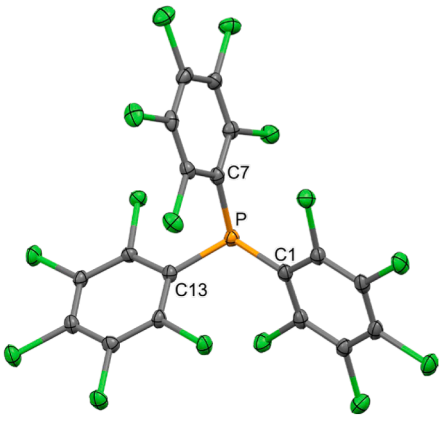

Fig. 1. Displacement-ellipsoid diagram (50% probability) of the *A* stereoisomer of the perchlorophenyl phosphine $(C_6Cl_5)_3P$ as found in single crystals of **1**. The *C* enantiomer is also present in the centrosymmetric crystal lattice. Selected bond lengths and angles are given in Table 1.

Table 1
Relevant distances [pm] and angles [°] in the perchlorophenyl derivatives $(C_6Cl_5)_3PE$ [E = nil (1), O (2), F_2 (3)] as determined by sc-XRD methods.[a]

	1[b]	**2**·C_2Cl_4[c]	**3**·PhMe[d]
P–E	—	146.7(2)	164.1(1)[e]
P–C(1)	184.7(3)	185.1(3)	184.6(3)
P–C(7)	185.0(3)	184.7(3)	184.7(4)
P–C(13)	185.8(3)	184.7(3)	184.6(3)[f]
P–C_3[g]	68.7(1)	62.9(1)	0.0[h]
C(1)–P–C(7)	110.4(1)	111.2(1)	119.9(1)
C(1)–P–C(13)	109.7(1)	105.9(1)	120.2(2)[f]
C(7)–P–C(13)	100.9(1)	108.0(1)	119.9(1)[f]
Σ(C–P–C')	321.0(1)	327.0(1)	360.0(1)
α_1	113.3(2)	115.4(2)	121.3(2)
α_2	116.2(2)	115.4(2)	121.2(2)
α_3	112.4(2)	117.2(2)	121.3(2)
β_1	129.5(2)	126.9(2)	121.9(2)[f]
β_2	126.6(2)	126.3(2)	121.2(2)
β_3	130.5(2)	125.7(2)	121.9(2)[f]
γ_1[i]	116.1(3)	117.5(3)	116.8(2)
γ_2[i]	116.5(3)	117.2(3)	117.6(3)
γ_3[i]	116.7(2)	116.9(2)	116.8(2)[f]
θ_1	106.1(1)	110.1(1)	90.1(1) / 89.6(1)[j]
θ_2	114.4(1)	108.0(1)	90.4(1) / 90.4(1)[j]
θ_3	115.4(1)	111.7(1)	89.6(1) / 90.1(1)[j]
φ_1	55.9(1)	45.4(1)	53.8(1)
φ_2	16.0(1)	57.4(1)	53.8(1)
φ_3	49.5(1)	35.2(1)	53.8(1)[f]
τ_1	8.0(1)	6.6(1)	2.4(1)
τ_2	9.9(1)	12.8(1)	0.0[h]
τ_3	7.1(1)	8.5(1)	2.4(1)[f]

[a] Angles defined in Fig. 2; those involving rings C(1)–C(6), C(7)–C(12) or C(13)–C(18) are indicated as ω_i (i = 1, 2, 3).
[b] Numbering scheme as in Fig. 1.
[c] Numbering scheme as in Fig. 4.
[d] Numbering scheme as in Fig. 5.
[e] Owing to the C_2 symmetry axis along the P–C(7) line, there is just an independent P–F moiety with a virtually linear F–P–F' unit: 179.2(1)°.
[f] In compound **3**, ring 3 is numbered C(1′)–C(6′) by symmetry.
[g] Distance of the P atom to the plane defined by the three C^{ipso} atoms.
[h] Imposed by symmetry.
[i] The C^o–C^{ipso}–$C^{o'}$ angles (γ) in every C_6Cl_5 ring are consistently narrower than 120° as is usually observed wherever the C_6X_5 groups (X = F, Cl) are bonded to metals of medium to low electronegativity: Ref [29].
[j] Angles involving the symmetry-related F and F' atoms are given.

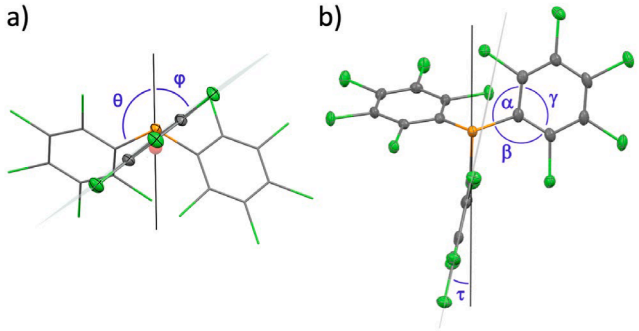

Fig. 2. Graphical definition of some angles used to describe the structure of the perchlorophenyl phosphine $(C_6Cl_5)_3P$ (**1**). The P lone-pair direction is taken as the line passing through the P atom and the centroid of the three C^{ipso} atoms (dummy atom in *a*). These angles equally apply to the $(C_6Cl_5)_3PO$ (**2**) and $(C_6Cl_5)_3PF_2$ (**3**) derivatives, where the axial direction is self-defined. Numerical values in all cases are given in Table 1.

the sum of angles around phosphorus, Σ(C–P–C'), as a useful criterion of pyramidality. This parameter, which is easily and unambiguously determined, is used as the primary measure of steric bulk. In the case of **1**, the fairly large value of Σ(C–P–C') 321.0(1)° shows evidence of significant steric crowding. This value nicely fits in the sequence of homologous Group 15 $(C_6Cl_5)_3Pc$ derivatives: Σ(C–P–C') 360.0° (N) [24], 321.0(1)° (P), 302.7(2)° (Sb) [23].

Boeré and Zhang distinguished between *steric protection* and *steric pressure* exerted by a given bulky group [5]. In the case of aryls, steric pressure is evidenced by a noticeable increase in Σ(C–P–C') (i.e., spreading of the pyramid) and only appears when bulky substituents are introduced in both *ortho* positions (2,6-disubstitution). Englert and his coworkers recently carried out a thorough classification of the structurally-characterized triarylphosphines according to the number of *ortho*-substituents, thereby providing a correlation between the C–P–C' angle and the P–C bond distance [30]. Aryl groups with bulky substituents in just one of the *ortho* sites (2-substitution) locate them in *exo* positions and result in steric protection of the P lone pair without significantly changing the Σ(C–P–C') value. This case is clearly illustrated by $\{2\text{-}(Me_3Si)C_6H_4\}_3P$ [30], which provides efficient protection to the P atom through the very bulky $SiMe_3$ substituents, but shows no spreading of the PC_3 pyramid, as indicated by the Σ(C–P–C') value 307.08(3)°, which is indistinguishable from that corresponding to unsubstituted Ph_3P: 307.3(1)° [31].

The steric pressure exerted by the C_6Cl_5 group is evidenced by the steady increase of the Σ(C–P–C') value along the $(C_6Cl_5)_nPh_{3-n}P$ series: 307.3(1)° (n = 0) [31] < 311.4(1)° (n = 1) [20] < 321.0(1)° (n = 3). In Table 2, the most relevant geometric features of the perchlorophenyl phosphine **1** are compared with those corresponding to representative examples of homoleptic 2,6-disubstituted triarylphosphines. The P–C bond length in **1** (185.2(3) pm av.) is in the long edge observed in related symmetric triarylphosphines (Table 2).

Given the characteristic structure of the perchlorophenyl phosphine **1**, we sought to evaluate its most fundamental properties, beginning with the calculation of the energy of its frontier orbitals. It has been suggested that the widening of the C–P–C' bond angles should result in increased p-character of the P lone-pair (HOMO), thereby rising its energy [32]. This destabilization, however, should be compensated (or even surpassed) in the case of the perchlorophenyl phosphine **1**, owing to the electron-withdrawing nature of the C_6Cl_5 group. The predominance of the latter effect is clearly seen by comparing the HOMO energy along the $(C_6Cl_5)_nPh_{3-n}P$ series (n = 0–3), where the gradual introduction of C_6Cl_5 groups results in steady HOMO stabilization (Table 3). Following our calculations, the perchlorophenyl phosphine **1** emerges as

Table 2
Relevant structural parameters of selected homoleptic 2,6-disubstituted triarylphosphines R_3P.

R	P–C [pm][a]	Σ(C–P–C') [°]	C–P–C' [°][a]	%V_{bur}[b]	Ref.
Ph[c]	183.2(3)	307.3(1)°	102.4(1)	31.1[d]	[31]
2,6-$Me_2C_6H_3$	184.2 (11)	328.6(6)	109.5(6)	42.1	[6]
Mes[c]	183.6(5)	328.7(2)	109.6(2)	41.6[d]	[7]
2,6-^{i}Pr$_2C_6H_3$ (Diip)	185.20 (15)	335.64(6)	111.87 (5)	–	[8]
2,4,6-^{i}Pr$_3C_6H_2$ (Tiip)	184.5(3)	334.4(1)	111.5(1)	–	[9]
4-NC-2,6-^{i}Pr$_2C_6H_2$	184.7(2)	335.0(1)	111.7(1)	–	[10]
4-MeO-2,6-^{i}Pr$_2C_6H_2$	185.0(1)	334.58(7)	111.53 (7)	–	[11]
4-Fc-2,6-^{i}Pr$_2C_6H_2$	185.4(2)	332.5(1)	110.8(1)	–	[12]
9-anthracenyl	183.9(4)	331.2(2)	110.4(2)	–	[14]
C_6F_5[d]	183.8(1)	311.4(1)	103.8(1)	35.7	[13]
2,6-$Cl_2C_6H_3$	183.3(3)	322.4(1)	107.5(1)	41.6	[32]
C_6Cl_5 (**1**)	185.2(3)	321.0(1)	107.0(1)	41.9	This work

[a] Average values indicated.
[b] Calculated from the corresponding $R_3P{-}Ni(CO)_3$ complex using the SambVca 2.1 online tool: Ref. [40a].
[c] Only the triclinic polymorph considered.
[d] Ref [41]. [e] Average values of the monoclinic and trigonal polymorphs.

Table 3
Characteristic parameters of the phosphines $(C_6Cl_5)_nPh_{3-n}P$ (n = 0–3), as estimated by calculation.[a]

	$n = 0$	$n = 1$	$n = 2$	$n = 3$	$(C_6F_5)_3P$ [a]
HOMO energy ($-I$) [E_h]	−0.1869[b]	−0.2367	−0.2504	−0.2590[c]	−0.2836 [d]
LUMO energy ($-A$) [E_h]	−0.0506[b]	−0.0656	−0.0754	−0.032	−0.0774
η [eV][e]	3.7[b]	4.66	4.76	4.78	5.61
inversion barrier [kcal mol^{-1}]	35.1[f]	24.6	21.3	17.1	26.7
proton affinity, PA [kJ mol^{-1}]	972.8[g]	919	895	878	800
aFIA [kJ mol^{-1}]	–	–	–	183	198
pF$^-$	–	–	–	4.4	4.7
%V_{bur} [h]	31.1[i]	34.4	37.4	41.9	35.7

[a] The perfluorophenyl phosphine $(C_6F_5)_3P$ is also included for comparison.
[b] Values taken from the Ligand Knowledge Base for Monodentate P-Donor Ligands (LKB-P): Ref [47].
[c] Calculated vertical / adiabatic detachment energy: 8.13 / 7.58 eV.
[d] Calculated vertical / adiabatic detachment energy: 9.05 / 8.56 eV.
[e] The HOMO–LUMO gap is identified as the chemical hardness, η: Ref. [33b].
[f] Ref [77].
[g] Experimental value from Ref [78].
[h] Calculated from the corresponding $R_3P{-}Ni(CO)_3$ complex using the SambVca 2.1 online tool: Ref. [40a].
[i] Ref [41].

a robust molecule characterized by a marked chemical hardness (η 4.78 eV) [33]. The still higher hardness calculated for the homologous perfluorophenyl phosphine $(C_6F_5)_3P$ (η 5.61 eV) can be ascribed to its more regular molecular structure with quite standard C–P–C' bond angles (Table 2).

Another consequence of the wider C–P–C' bond angles in **1** is its diminished inversion barrier (17.1 kcal mol^{-1}) when compared to other less encumbered triaylphosphines (Table 3). This comparatively low inversion barrier might well underlie the broad signals observed in the ^{13}C NMR spectrum of **1** in solution with not well-resolved coupling to P. Hindered rotation around the P–C bond might also contribute to the observed broadening.

Mass spectrometric (MS) experiments on **1** provide evidence of reactivity in two important kinds of processes directly involving the P lone-pair (HOMO): a) one-electron oxidation, and b) protonation (Scheme 3). Compound **1** proved to be difficult to ionize using various techniques. When running FAB+ experiments, a low-intensity peak corresponding to the radical cation $[(C_6Cl_5)_3P^{\bullet}]^+$ (m/z = 772) is observed, in keeping with an early report [22]. The ionization process undergone by **1** in the gas phase was examined by calculation, giving a vertical / adiabatic detachment energy of 8.13 / 7.58 eV. Still higher energies were calculated for the perfluorophenyl homologue $(C_6F_5)_3P$: 9.05 / 8.56 eV. In contrast, the vertical ionization potential experimentally established for the unsubstituted Ph_3P amounts 7.8 eV [34]. The observed shift along the $(C_6X_5)_3P$ series (X = H, Cl, F) is in keeping with their corresponding HOMO energies (Table 3). The optimized geometry of the radical cation $[(C_6Cl_5)_3P^{\bullet}]^+$ (Fig. S1b), is still pyramidal, but considerably more flattened, Σ(C–P–C') 353.5°, than the parent neutral phosphine **1**. This significant flattening has been observed in previous instances, as in various salts of the $[(Mes)_3P^{\bullet}]^+$ and $[(Tipp)_3P^{\bullet}]^+$ cations [35], meaning that the SOMO has enhanced p character. The spin-density distribution shows that the unpaired electron in the $[(C_6Cl_5)_3P^{\bullet}]^+$ cation is located mainly on the P atom with just slight delocalization onto the aryl rings (Fig. 3).

When the MS experiments are carried out using the APCI technique, much stronger peaks were observed, with the major one corresponding to the protonated phosphine $[(C_6Cl_5)_3PH]^+$ (m/z = 773). Following this experimental result (Scheme 3), the proton affinity of **1** in the gas phase (PA) was estimated by calculation. The obtained value (PA 878 kJ/mol) shows that **1** is the least basic phosphine within the $(C_6Cl_5)_nPh_{3-n}P$ series (n = 0–3; Table 3) [36] in keeping with the electron-withdrawing character of the C_6Cl_5 group. We note that the homologous perfluorophenyl phosphine $(C_6F_5)_3P$ is considerably less basic (PA 800 kJ/mol), suggesting that the group electronegativities of C_6F_5 and C_6Cl_5 are actually more different than it has been traditionally considered [15]. Probably the least basic of all homoleptic organophosphines is the trifluoromethyl phosphine $(CF_3)_3P$, which cannot be protonated —not even by HF/SbF_5—, but can still be methylated to $[(CF_3)_3PMe]^+$ [37].

The most marked difference between the perhalophenyl phosphines $(C_6X_5)_3P$ (X = F, Cl) is certainly their respective size. From the various means to evaluate this essential feature [38], we have chosen to rely on the recently introduced buried volume, %V_{bur}, as a convenient way to assess the steric requirement of a given molecule or molecular fragment. It can be considered as an extension of the cone angle originally formulated by Tolman [39], but is not limited to any particular geometry. In fact, this versatile parameter applies to a wide variety of systems including all kinds of phosphines and NHC ligands (Lewis bases) [40]. Recently, it has also been used to evaluate the steric properties of Lewis acids [41]. The perchlorophenyl phosphine **1** is the bulkiest of the $(C_6Cl_5)_nPh_{3-n}P$ series (n = 0–3), with %V_{bur} steadily increasing along the series (Table 3) from 31.1 (n = 0) [41] to 41.9 (n = 3). The steric bulk of **1** is comparable to those of the homoleptic R_3P phosphines with R = Mes, 2,6-$Me_2C_6H_3$, and 2,6-$Cl_2C_6H_3$, all with %V_{bur} ≈ 42 (Table 2). These phosphines (including **1**) build an interesting set of ligands with virtually the same steric hindrance towards the acceptor center, but with diverse electronic properties depending on the number and the nature of the substituents.

Phosphines, especially those with electron-withdrawing substituents, usually exhibit amphoteric character. As typical examples, the hypervalent $[PX_4]^-$ phosphoranides (X = F, Cl, Br) are formed by interaction of PX_3 with a QX salt (Q^+ being a poorly electrophilic cation) [42]. This Lewis-acidic behavior has also been observed with organophosphines bearing perfluoroalkyl groups, as $(CF_3)_3P$ [43], $(CF_3CF_2)_3P$

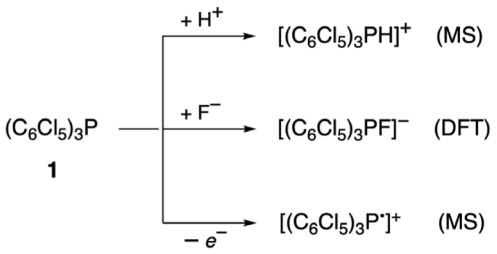

Scheme 3. Fundamental processes characteristic of the perchlorophenyl phosphine **1**. The energy involved in each process has been calculated by DFT methods (Table 3).

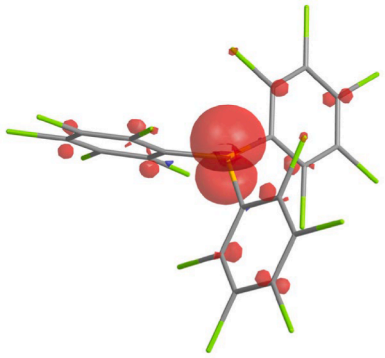

Fig. 3. Spin density contour (isovalue 0.004) of the radical cation $[(C_6Cl_5)_3P^{\bullet}]^+$ in the gas phase. The geometry was optimized at the DFT/M06 level of theory (Fig. S1b).

[44], or $(CF_3CF_2)_2PF$ [45]. A simple way to assess the potential role of the perchlorophenyl phosphine **1** as a Lewis acid consists in calculating its fluoride ion affinity (FIA) to give the anionic phosphoranide $[(C_6Cl_5)_3PF]^-$ (Scheme 3). The enthalpy involved in the associative process shown in Eq. (1a), where **A** denotes the Lewis acid, is the raw FIA value with opposite sign by convention.

$$\mathbf{A} + F^- \longrightarrow [\mathbf{AF}]^- \qquad \Delta H = -\mathrm{FIA} \qquad (1a)$$

$$\mathbf{A} + CF_3O^- \longrightarrow [\mathbf{AF}]^- + COF_2 \qquad \Delta H = -\mathrm{aFIA} \qquad (1b)$$

By incorporating CF_2O as a fluoride carrier to the calculation (Eq. 1b), as suggested by Christe [46], the so-called absolute FIA (aFIA) is obtained given that the enthalpy of the subsystem $CF_2O + F^- \longrightarrow CF_3O^-$ is experimentally known. Christe further introduced the pF^- value, defined as $pF^- = -\mathrm{aFIA}$ (in kcal mol^{-1})/10. The pF^- of the perchlorophenyl phosphine **1** is 4.4, which is comparable to that corresponding to PF_3 (4.5) [46]. In view of these similar values, it might be foreseen that the anionic phosphoranide $[(C_6Cl_5)_3PF]^-$ might be obtained under the suitable experimental conditions and using a poorly electrophilic cation in analogy to the known $Q[PF_4]$ salts [42a].

2.2. The phosphine oxide $(C_6Cl_5)_3PO$ (2)

Whereas trialkyl phosphines react with O_2, even violently, to give the corresponding oxides, triarylphosphines are much less reactive towards oxygen. Thus, the unsubstituted archetype Ph_3P is not particularly air-sensitive. This lower reactivity, which is sometimes an advantageous feature enabling easy handling, is due to both steric and electronic factors. The introduction of electron-withdrawing substituents lowers the HOMO energy and renders the phosphorus less basic [36,47]. For this reason, the deactivated perfluorophenyl phosphine $(C_6F_5)_3P$, for instance, requires harsh conditions to get oxidized, *e.g.* $Na_2Cr_2O_7$ in strongly acidic medium [48], or use of the nitroxyl $(CF_3)_2NO^\bullet$ reagent [49]. On the other hand, the introduction of bulky *ortho*-substituents further enhances the stability of triarylphosphines towards air oxidation [50]. In this regard, the extremely crowded phosphines $(Dipp)_3P$ [8] and $(Tipp)_3P$ [9] are also air-stable and do not get oxidised with H_2O_2 (at least under the essayed conditions) in spite of the electron-donor nature or the ^{i}Pr substituents. Nevertheless, the latter was eventually transformed into the corresponding oxide $(Tipp)_3PO$ by treatment with *m*-chloroperoxybenzoic acid (mCPBA) [51]. Considering all these precedents, it can be envisaged that the perchlorophenyl phosphine **1** will not be readily oxidized, because it represents the less favorable combination of factors: 1) full aryl substitution with strongly electron-withdrawing Cl atoms, and 2) steric shielding of the P atom by the quite bulky *ortho*-substituents. In fact, all the phosphine oxides in the series $(C_6Cl_5)_nPh_{3-n}PO$ (n = 0–3) are already known, except right that with n = 3 [21].

The phosphine oxide $(C_6Cl_5)_3PO$ (**2**) was prepared by prolonged treatment of the parent phosphine **1** with H_2O_2 in boiling toluene (Scheme 2) and was isolated as a white solid in 61.5% yield. It was characterized by analytic, spectroscopic and structural methods. The IR spectrum of **2** shows typical absorptions associated to the C_6Cl_5 group. The frequency of the so-called X-sensitive vibration mode [28] appears shifted from 865 in cm^{-1} in the parent phosphine **1** to 881 cm^{-1} in the phosphine oxide **2**, in keeping with the oxidation-state increase [23,52]. The absorption corresponding to ν(PO) would be expected to appear at about 1200 cm^{-1} by analogy to other related phosphine oxides [21]. This absorption, however, probably overlaps with absorptions of the C_6Cl_5 group in the same region and could not be unambiguously located. The ^{31}P NMR signal undergoes a considerable downfield shift upon oxidation, moving from δ_P 9.6 ppm in the parent phosphine **1** to δ_P 23.6 ppm in the oxide **2**.

The crystal and molecular structures of **2** have been established by sc-XRD methods. The molecular structure is shown in Fig. 4 and selected interatomic distances and angles are given in Table 1. The overall

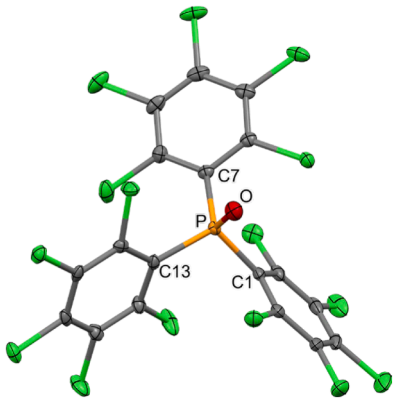

Fig. 4. Displacement-ellipsoid diagram (50% probability) of the *C* stereoisomer of the phosphine oxide $(C_6Cl_5)_3PO$ as found in single crystals of **2**·C_2Cl_4. The *A* enantiomer is also present in the centrosymmetric crystal lattice. Selected bond lengths and angles are given in Table 1.

geometry can be described as trigonal pyramidal (*TPY*-4) with the oxygen atom located in the apical position. The most relevant structural parameters of **2** are compared in Table 4 with those observed in related triarylphosphine oxides R_3PO [51,53–55]. The stereochemistry of the unsubstituted product Ph_3PO was thoroughly analyzed by Dunitz *et al.* [56]. The base of the pyramid in **2** is slightly spread with respect to the parent phosphine **1** as shown by the wider Σ(C–P–C') value: 327.0(1)° (in **2**) vs. 321.0(1)° (in **1**). The P–C bond lengths in **2** (184.8(3) pm av.) are comparable to those found in the parent phosphine **1** (185.2(3) pm av.) in spite of the different oxidation state of P in each case. The flattening of the pyramid while maintaining comparable P–C distances results in diminishing the separation of the P atom from the basal plane: P–C_3 62.9(1) pm (in **2**) vs. 68.7(1) pm (in **1**). The presence of the apical O atom generates even greater steric pressure, which is somewhat released by reorienting the C_6Cl_5 rings to the most suitable positions. They are tilted in **2** an average angle of φ 46.0(1)° (Table 1) with less dispersion than in **1** (φ 40.5° av.). The P–O bond length, 146.7(2) pm, is in the lower edge of the related R_3PO precedents (Table 4), being identical to that observed in the perfluorophenyl homologue $(C_6F_5)_3PO$ [55]. The short P–O distance is ascribed to the electron-withdrawing effect of the C_6X_5 groups (X = F, Cl) [15] and should render the O atom less basic. In the case of **2**, however, the terminal O atom is sufficiently basic to get protonated in the gas phase (Scheme 4). In fact, the most abundant peak in the MS of **2** using the atmospheric pressure chemical ionization (APCI+) technique is that corresponding to the cation $[(C_6Cl_5)_3POH]^+$ (m/z = 789). Following our estimates, the oxide **2** is slightly more basic than the parent phosphine **1**, with PA values of 884.5 *vs.* 878, respectively. It also shows slightly increased Lewis acidity as indicated by the corresponding pF^- values: 4.9 (in **2**) vs. 4.4 (in **1**).

The steric crowding in **2** is further evidenced by the presence of six

Table 4
Relevant structural parameters of representative triarylphosphine oxides R_3PO.

R	P–O [pm]	P–C [pm][a]	O–P–C [°][a]	Σ(C–P–C') [°]	φ [°][a,b]	Ref.
Ph	147.9 (2)	180.3 (1)	112.6(1)	318.6(1)	31.5 (1)	[53]
Mes	148.6 (2)	182.8 (3)	108.7(1)	330.4(1)	44.1 (1)	[54]
Tiip	148.1 (2)	185.1 (2)	106.8(1)	336.0(1)	41.4 (1)	[51]
C_6F_5	146.7 (2)[a]	181.7 (2)	112.9(1)	317.4(1)[a]	32.1 (1)	[55]
C_6Cl_5 (**2**)	146.7 (2)	184.8 (4)	109.9(1)	327.0(1)	46.0 (1)	This work

[a] Average value indicated.
[b] Angle φ as defined in Fig. 2.

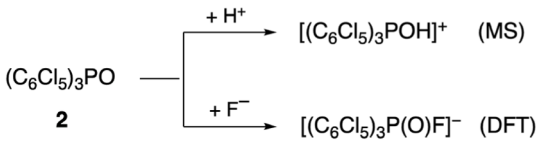

Scheme 4. Fundamental processes characteristic of the phosphine oxide **2**. The energy involved in each process has been calculated by DFT methods (see discussion).

signals in its ^{13}C NMR spectrum. This means that the rotation or the aryl groups around the P–C bond is hindered in the NMR time-scale leaving all six C atoms of the C_6Cl_5 rings inequivalent. All the signals appear in the aromatic region (138.2–128.5 ppm) and show well-resolved coupling to the central P atom with different $^nJ(^{31}P,^{13}C)$ values, the largest one involving the C^{ipso} atom: $^1J(^{31}P,^{13}C) = 120.3$ Hz.

Compound **2** completes the series of phosphine oxides with general formula $(C_6Cl_5)_nPh_{3-n}PO$ (n = 0–3) [21], also being the most sterically encumbered member of the series. We speculated whether it might be possible to increase the steric pressure a step further by increasing the number of substituents bound to P (expanding its coordination number in terms of coordination chemistry). This possibility was fulfilled with the synthesis of the difluorophosphorane $(C_6Cl_5)_3PF_2$ (**3**), as we will discuss next.

2.3. *The difluorophosphorane $(C_6Cl_5)_3PF_2$ (3)*

In view of the harsh conditions required to prepare the phosphine oxide **2**, we anticipated that the transformation of **1** into **3** might likewise require energetic conditions. In this particular case, however, the effective experimental settings are limited by two negative factors: 1) the low solubility of **1** in common organic media, and 2) the limited tolerance of most organic solvents towards the fluorinating agent XeF_2 at high temperature [57]. In order to overcome these important drawbacks, we carried out the reaction at high temperature in the absence of any kind of solvent. The solvent-free reaction of the perchlorophenyl phosphine **1** with XeF_2 in a teflon tube at 110 °C for 48 h actually afforded compound **3** (Scheme 2), which was isolated as a pale-yellow solid in 85% yield. It was characterized by analytic, spectroscopic and structural methods. With the synthesis of **3**, the series of difluorophosphoranes with general formula $(C_6Cl_5)_nPh_{3-n}PF_2$ (n = 0–3) [20, 58] is now complete.

In the IR spectrum of **3**, the strong absorption at 768 cm^{-1} is assigned to the $\nu_{as}(PF_2)$ vibration mode [59]. This frequency is comparable to that observed for the homologous perfluorophenyl derivative $(C_6F_5)_3PF_2$ (765 cm^{-1} in Nujol; 773 cm^{-1} in HCy solution) [59]. The high value observed can be ascribed to the high group electronegativity, which is comparable in both cases [15]. In line with this reasoning is the still higher frequency observed for the trifluoromethyl difluorophosphorane $(CF_3)_3PF_2$ (855 cm^{-1}) [59]. In the IR spectrum of **3**, the so-called X-sensitive vibration mode of the C_6Cl_5 group appears at 885 cm^{-1}, being the highest frequency observed in the set of compounds **1**–**3**.

The ^{31}P NMR spectrum of **3** shows a triplet at δ_P −40.70 ppm with strong coupling to the two incorporated F atoms: $^1J(^{19}F,^{31}P) = 782.1$ Hz. The ^{19}F NMR spectrum, in turn, consists of a doublet at δ_F −14.45 ppm with the same coupling constant, indicating that the two F atoms are equivalent. The NMR spectroscopic parameters of **3** are compared in Table 5 with those reported for the other members of the $(C_6Cl_5)_nPh_{3-n}PF_2$ series (n = 0–3) [20,58] In this comparison, we see that the gradual incorporation of C_6Cl_5 groups results in downfield shifts of δ_P and δ_F, which is steady in the case of δ_P and slightly less regular in the case of δ_F. The $^1J(^{19}F,^{31}P)$ value also shows a regular increase with the gradual introduction of C_6Cl_5 groups: from 660 Hz (n = 0) to 782.1 Hz (n = 3). The presence of just four signals in the ^{13}C NMR spectrum of **3** indicates high molecular symmetry.

The molecular structure of **3**, as established by sc-XRD methods, is shown in Fig. 5. The overall geometry can be described as trigonal bipyramidal (*TBPY*-5) with axial fluorine atoms. Relevant structural parameters are given in Table 1. They are compared in Table 6 with those corresponding to related triaryl difluorophosphoranes R_3PF_2 [58, 60–64]. In the crystal, a binary axis crosses the molecule along the P–C (7) bond. Accordingly, only half of the molecule is independent, the other half being generated by symmetry. The axial F–P–F' unit is virtually linear, 179.2(1)°, as generally found in related R_3PF_2 molecules (Table 6). The P–F bond length in **3** (164.1(1) pm) is in the lower edge, being indistinguishable within the experimental error from those found in other difluorophosphoranes with electron-withdrawing aryls, such as C_6F_5, 4-CNC_6F_4 or 3,5-$(CF_3)_2C_6H_3$. In contrast, the average P–C bond length in **3** (184.6(4) pm) is in the upper edge, being, in turn, indistinguishable from that found in $(Mes)_3PF_2$: 184.7(6) pm. It seems that in R_3PF_2 molecules, the F–P–F axis is governed mainly by electronic factors of the aryl substituents, whereas their steric factors have more impact on the equatorial PC_3 plane.

The C_6Cl_5 groups in **3** are all twisted by 53.8(1)° with respect to the F–P–F' axis (Table 6). The marked twist together with the P–C elongation contribute to minimize the steric pressure in this overcrowded molecule with intramolecular *ortho*-Cl···F non-bonded distances of ca. 285 pm [65,66]. It is worth noting that, in the mixed aryl difluorophosphorane $(C_6Cl_5)Ph_2PF_2$ [20], the C_6Cl_5 ring is also much more twisted (60°) with respect to the F–P–F' axis than the unsubstituted Ph rings (27° and 32°). Moreover, the P–C_6Cl_5 bond is also elongated with respect to the P–Ph bonds within the same molecule: 185.2(1) vs. 181.9 (1) and 182.1(1) pm.

The geometry of **3** in the gas phase, as optimized by calculation (Fig.

Table 5
Spectroscopic and structural parameters of the difluorophosphoranes $(C_6Cl_5)_nPh_{3-n}PF_2$ (n = 0–3).

	$n = 0$[a]	$n = 1$[b]	$n = 2$[b]	$n = 3$[c]
δ_P [ppm]	−55.0	−50.69	−44.91	−40.70
δ_F [ppm]	−39.6	−41.79	−28.9	−14.45
$^1J(^{19}F,^{31}P)$ [Hz]	660	715.5	746.5	782.1
$\nu_{as}(PF_2)$ [cm^{-1}]	~680[d]	–	–	768
P–F [pm]	166.3(2)	166.0(1)[e]	–	164.1(1)
F–P–F' [°]	178.3(2)	175.94(5)	–	179.2(1)
Σ(C–P–C') [°]	360.0(2)	360.0(1)	–	360.0(1)

[a] Ref [64].
[b] Ref [20].
[c] This work.
[d] The asymmetric PF_2 stretching frequency is dependent on the sample preparation: 670 cm^{-1} in Nujol, 690 cm^{-1} in CyH solution.
[e] Average value indicated.

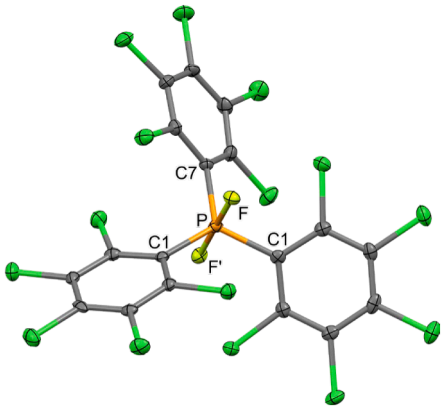

Fig. 5. Displacement-ellipsoid diagram (50% probability) of the *A* stereoisomer of the difluorophosphorane $(C_6Cl_5)_3PF_2$ as found in single crystals of **3**·PhMe. The *C* enantiomer is also present in the centrosymmetric crystal lattice. Selected bond lengths and angles are given in Table 1.

Table 6
Relevant structural parameters of representative triaryl difluorophosphoranes R_3PF_2.

R	P–F [pm]	P–C [pm][a]	F–P–F' [°]	Σ(C–P–C') [°]	φ [°][a,b]	Ref.
Ph	166.3(2)	182.5(6)	178.3(2)	360.0(2)	30.6	[58]
4-ClC_6H_4[c]	167.0(1)[a]	181.8(2)	176.7(1)[a]	360.0(1)[a]	29.6	[60]
3,5-$(CF_3)_2C_6H_3$	164.5(1)	181.7(3)	179.7(1)	360.0(1)	21.1	[61]
Mes	167.3(2)	184.7(6)	179.6(2)	359.9(2)	48.5	[62]
C_6F_5	163.6(2)	181.8(4)	180.0	360.1(2)	53.5	[63]
4-CNC_6F_4	163.8(1)[a]	181.6(2)	178.1(1)	360.0(1)	54.2	[64]
C_6Cl_5 (**3**)	164.1(1)	184.6(4)	179.2(1)	360.0(1)	53.8(1)	This work

[a] Average values indicated.
[b] Angle φ as defined in Fig. 2.
[c] Two independent molecules in the unit cell.

S1f), has even higher symmetry with all three C_6Cl_5 rings equivalent (effective D_3 symmetry). This structure is compatible with the observed ^{13}C NMR spectrum of **3** in solution consisting of just four signals with different coupling constants to the central P atom —the largest one being that corresponding to the C^{ipso} atoms: $^1J(^{13}C,^{31}P) = 213.9$ Hz.

In the MS of **3** (MALDI+), the major peak corresponds to the $[(C_6Cl_5)_3PF]^+$ cation ($m/z = 791$) formed by dissociation of a fluoride ion (Scheme 5). This is the reverse process of that shown in Eq. (1a), with the fluorophosphonium cation $[(C_6Cl_5)_3PF]^+$ being the Lewis acid and the difluorophosphorane **3** its conjugate Lewis base.

The structure of the fluorophosphonium cation $[(C_6Cl_5)_3PF]^+$ has been optimized by calculation (Fig. S1h) and its Lewis acidity has also been estimated. The pF^- value obtained (15.8) clearly surpasses that corresponding to SbF_5 (12.0) and hence it can be ranked as a Lewis superacid according to Krossing's criterion [67]. Recently, Radius, Finze and their coworkers, quantified the steric properties of a given Lewis acid A by calculating the $\%V_{bur}$ of its conjugate base $[AF]^-$ [Eq. (1a)] [41]. In the case of the fluorophosphonium cations $[(C_6X_5)_3PF]^+$ (X = F [68], Cl), this procedure can be applied using directly the experimental structures of the corresponding difluorophosphoranes $(C_6X_5)_3PF_2$ (Table 6), whereby the following $\%V_{bur}$ values are obtained: 63.2 (X = F) vs. 71.3 (X = Cl). This significant difference makes apparent that the acidic site is much more protected in the $[(C_6Cl_5)_3PF]^+$ case. The efficient shielding exerted by the C_6Cl_5 groups should result in higher selectivity of the perchlorophenyl cation $[(C_6Cl_5)_3PF]^+$ towards the incoming base.

The difluorophosphorane **3** itself exhibits Lewis acidity, showing enhanced affinity for an additional F^- ligand ($pF^- = 6.3$). The corresponding conjugate base has octahedral structure with meridional geometry, [*mer*-$(C_6Cl_5)_3PF_3]^-$, as optimized by calculation (Fig. S1g). The structure of this hypervalent derivative bears much similarity to that experimentally established for its perfluorophenyl homologue in the [K([18]crown-6)][*mer*-$(C_6F_5)_3PF_3$] salt, which was recently prepared by Hoge and his coworkers [64]. The appreciably higher pF^- value calculated for the perfluorophenyl difluorophosphorane $(C_6F_5)_3PF_2$ Lewis acid ($pF^- = 7.6$) [64] again suggests that the C_6F_5 group is more electron-withdrawing than C_6Cl_5.

3. Conclusion

The perchlorophenyl phosphine $(C_6Cl_5)_3P$ (**1**) exhibits pyramidal structure, yet considerably flattened by the steric pressure exerted by the bulky C_6Cl_5 groups. The structure is intermediate between the trigonal planar amine $(C_6Cl_5)_3N$ [24] and the more regular pyramidal stibine $(C_6Cl_5)_3Sb$ [23]. The most fundamental properties of this unusual phosphine have been captured by theoretical methods. Following our calculations, $(C_6Cl_5)_3P$ (**1**) emerges as a sterically encumbered phosphine with amphoteric character, showing diminished basicity towards electrophiles (low proton affinity, PA) and increased Lewis acidity (moderate fluoride ion affinity, FIA). The protective effect of the C_6Cl_5 groups (large $\%V_{bur}$ value) together with the marked chemical hardness (η 4.78 eV) render this unusual phosphine rather stable and chemically unreactive. This chemical inertness notwithstanding, it has been possible to bring it into reaction under harsh conditions to afford its oxide $(C_6Cl_5)_3PO$ (**2**) and the corresponding difluorophosphorane $(C_6Cl_5)_3PF_2$ (**3**).

The P centre is increasingly protected by the ligands along the series **1** < **2** < **3**, as clearly seen in Fig. 6. The phosphine oxide **2** is more basic than its parent phosphine **1**, both being protonated in the gas phase to the corresponding cations $[(C_6Cl_5)_3PH]^+$ and $[(C_6Cl_5)_3POH]^+$. The difluorophosphorane $(C_6Cl_5)_3PF_2$ (**3**) releases one of the axial fluorides in the gas phase giving the fluorophosphonium cation $[(C_6Cl_5)_3PF]^+$, which is a Lewis superacid. The high value of $\%V_{bur}$ evidences that the acidic σ* hole is strongly shielded. Consequently, this cation might well exhibit high selectivity towards the incoming nucleophile.

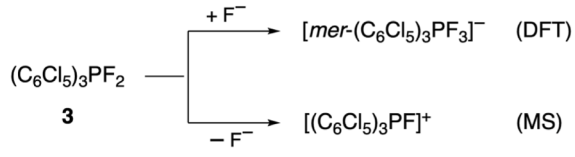

Scheme 5. Amphoteric character of the difluorophosphorane **3**. The energy involved in each process has been calculated by DFT methods (see discussion).

4. Experimental section

4.1. General procedures and materials

Unless otherwise stated, the reactions and manipulations were carried out under purified argon using Schlenk techniques. Solvents were dried using an MBraun SPS-800 System. Ether solutions of LiC_6Cl_5 were obtained at low temperature as described elsewhere [69]. Samples of PCl_3 were purchased from a commercial source (Sigma-Aldrich) and used as received. Elemental analyses were carried out using a Perkin Elmer 2400 CHNS/O Series II microanalyzer. IR spectra were recorded on KBr disks using a Perkin-Elmer Spectrum-100 FT-IR spectrometer (4000–250 cm^{-1}). Multinuclear NMR spectra (^{13}C, ^{19}F and ^{31}P) were recorded at room temperature on Bruker ARX 300 or AV 400 spectrometers. Chemical shifts of the measured nuclei (δ in ppm) are given with respect to the standard references in use: $SiMe_4$ (δ_C), $CFCl_3$ (δ_F) and 85% aqueous H_3PO_4 (δ_P). Mass spectra (MS) were registered using

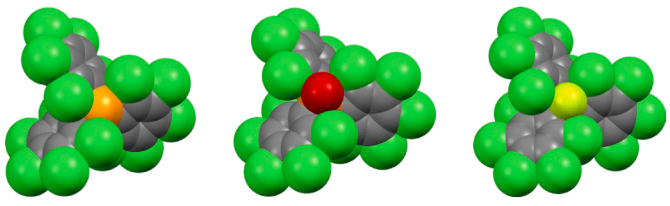

Fig. 6. Space-filling drawing of the perchlorophenyl derivatives $(C_6Cl_5)_3P$ (**1**; left), $(C_6Cl_5)_3PO$ (**2**; center) and $(C_6Cl_5)_3PF_2$ (**3**; right) with atoms in their standard colors.

different techniques and ionization methods with the indicated equipment: (a) matrix-assisted laser desorption/ionization time-of-flight (MALDI-TOF) under positive detection on Bruker MicroFlex or AutoFlex spectrometers, (b) fast atom bombardment (FAB) under positive detection on a VG-Autospec spectrometer operating at ca. 35 kV and using the standard Cs^+ ion gun, (c) atmospheric pressure chemical ionization (APCI) under positive detection on a Bruker Esquire 3000+ spectrometer.

4.2. Synthesis of $(C_6Cl_5)_3P$ (1)

The dropwise addition of a solution of PCl_3 (0.5 cm^3, 5.73 mmol) in Et_2O (15 cm^3) at −78 °C onto another solution of previously formed LiC_6Cl_5 (23 mmol) in Et_2O (70 cm^3) under stirring caused the immediate precipitation of an off-white solid. The reaction medium was allowed to warm slowly while stirring. When the temperature reached 0 °C, the suspension was maintained in an ice bath under good stirring for additional 15 h and then filtered. The off-white solid was washed with MeOH (3 × 10 cm^3) and vacuum dried. It was identified as $(C_6Cl_5)_3P$ (3.18 g, 4.1 mmol, 71.2% yield). **IR** (KBr): $\tilde{\nu}/cm^{-1}$ = 1513 (m), 1441 (w), 1337 (vs), 1325 (vs), 1301 (vs), 1220 (m), 1165 (m), 1094 (m), 878 (m), 865 (s; C_6Cl_5: X-sensitive vibration) [28], 688 (s), 619 (m), 586 (w), 427 (m). **^{13}C NMR** (100.577 MHz, $(CH_2Cl)_2/CD_2Cl_2$): δ_C/ppm = 137.1, 136.8, 135.6, 134.2, 133.8, 133.0. **^{31}P NMR** (121.442 MHz, $(CH_2Cl)_2/CD_2Cl_2$): δ_P/ppm = 9.6. **MS** (FAB+): m/z = 772: $[(C_6Cl_5)_3P]^+$ (low intensity). **MS** (APCI+): m/z = 773: $[(C_6Cl_5)_3PH]^+$. **Elemental analysis** calcd (%) for $C_{18}Cl_{15}P$: C 27.75; found: C 27.7.

Single crystals suitable for X-ray diffraction purposes were obtained by allowing a saturated solution of **1** in CCl_4 at 80 °C to cool down very slowly to 3 °C.

4.3. Synthesis of $(C_6Cl_5)_3PO$ (2)

To a solution of **1** (0.2 g, 0.26 mmol) in boiling toluene (25 cm^3), seven portions of H_2O_2 (33%) were regularly added (0.1 cm^3 each, 0.7 cm^3 total) along 20 h of reflux, after which time, the solvent was evaporated in vacuo. By treating the resulting residue with MeOH (10 cm^3), a white solid was obtained, which, after filtering and drying, was identified as $(C_6Cl_5)_3PO$ (0.13 g, 0.16 mmol, 61.5% yield). **IR** (KBr): $\tilde{\nu}/cm^{-1}$ = 1514 (m), 1331 (s), 1306 (vs), 1224 (m), 1168 (m), 1102 (m), 1029 (w), 881 (s; C_6Cl_5: X-sensitive vibration) [28], 805 (w), 722 (w), 693 (m), 676 (w), 623 (m), 602 (w), 457 (s), 395 (w), 371 (w). **^{13}C NMR** (100.577 MHz, CD_2Cl_2): δ_C/ppm = 138.2 [d, $^4J(^{31}P,^{13}C)$ = 3.0 Hz; C^p], 136.2 [d, $^2J(^{31}P,^{13}C)$ = 93.5 Hz; C^o], 135.1 [d, $^2J(^{31}P,^{13}C)$ = 96.2 Hz; C^o], 133.3 [d, $^1J(^{31}P,^{13}C)$ = 120.3 Hz; C^{ipso}], 133.4 [d, $^3J(^{31}P,^{13}C)$ = 58.1 Hz; C^m], 128.5 [d, $^3J(^{31}P,^{13}C)$ = 59.8 Hz; C^m]. **^{31}P NMR** (161.923 MHz, CD_2Cl_2): δ_P/ppm = 23.6. **MS** (APCI+): m/z = 789: $[(C_6Cl_5)_3POH]^+$. **Elemental analysis** calcd (%) for $C_{18}Cl_{15}OP$: C 27.2; found: C 27.8.

Single crystals of **2**·C_2Cl_4 suitable for X-ray diffraction purposes were obtained by allowing a saturated solution of **2** in C_2Cl_4 at 80 °C to cool down very slowly to 3 °C.

4.4. Synthesis of $(C_6Cl_5)_3PF_2$ (3)

In a Teflon tube, a solid sample of **1** (0.1 g, 0.13 mmol) was mixed at room temperature with an excess of solid XeF_2 (0.06 g, 0.35 mmol). Once the Teflon tube was closed, it was located in an oven and warmed at 110 °C for 48 h. After cooling down, the initial mixture had transformed into a pale-yellow solid, which was identified as $(C_6Cl_5)_3PF_2$ (94 mg, 0.11 mmol, 85% yield). **IR** (KBr): $\tilde{\nu}/cm^{-1}$ = 1515 (m), 1389 (w), 1334 (s), 1310 (s), 1205 (w), 1177 (m), 1103 (m), 885 (s; C_6Cl_5: X-sensitive vibration) [28], 768 [s; $\nu_{as}(PF_2)$], [59], 725 (w), 686 (m), 628 (w), 608 (w), 497 (s). **^{13}C{^{19}F} NMR** (73.432 MHz, CCl_4/CD_2Cl_2): δ_C/ppm = 137.0 [d, $^4J(^{31}P,^{13}C)$ = 2.8 Hz; C^p], 135.8 [d, $^1J(^{31}P,^{13}C)$ = 213.9 Hz; C^{ipso}], 134.8 [d, $^3J(^{31}P,^{13}C)$ = 94.6 Hz; C^m], 134.6 [d, $^2J(^{31}P,^{13}C)$ = 116.1 Hz; C^o]. **^{19}F NMR** (282.231 MHz, CD_2Cl_2): δ_F/ppm = −14.45 [d, $^1J(^{19}F,^{31}P)$ = 782.1 Hz]. **^{31}P NMR** (121.442 MHz, CD_2Cl_2): δ_P/ppm = −40.70 [t, $^1J(^{19}F,^{31}P)$ = 782.1 Hz). **MS** (MALDI+): m/z = 791: $[(C_6Cl_5)_3PF]^+$ (major), 772: $[(C_6Cl_5)_3P]^+$, 561: $[(C_6Cl_5)_2PF_2]^+$, 525: $[(C_6Cl_5)_2P]^+$. **Elemental analysis** calcd (%) for $C_{18}Cl_{15}F_2P$: C 26.5; found: C 26.3.

Single crystals of **3**·PhMe suitable for X-ray diffraction purposes were obtained by allowing a saturated solution of **3** in toluene at 80 °C to cool down very slowly to 3 °C.

4.5. X-Ray structure determinations

Crystal data and other details of the structure analysis are presented in Table 7. Suitable single crystals were obtained as indicated in the corresponding experimental entry. Crystals were mounted on quartz fibres in random orientation and held in place with fluorinated oil. Diffraction data were collected at 100 K on an Oxford Diffraction Xcalibur CCD diffractometer using graphite-monochromated Mo-Kα (λ = 71.073 pm) radiation. The obtained diffraction frames were integrated and corrected for absorption using the CrysAlis RED package [70]. Lorentz and polarisation corrections were applied for all the structures.

The structures were solved by Patterson and direct methods. All non-hydrogen atoms of the organophosphorus species were assigned anisotropic displacement parameters. The hydrogen atoms were constrained to idealised geometries and assigned isotropic displacement parameters equal to 1.2 or 1.5 times the U_{iso} values of their respective parent atoms. For **3**·PhMe, the interstitial toluene molecule lies near a symmetry element and its atoms were refined with 0.5 occupancy; the involved C–C distances were restrained to suitable values. Full-matrix least-squares refinement of these models against F^2 using the SHELXL-97 program [71] converged to final residual indices given in Table 7.

Table 7
Crystal data and structure refinement for compounds **1**, **2**·C_2Cl_4 and **3**·PhMe.

	1	**2**·C_2Cl_4	**3**·PhMe
formula	$C_{18}Cl_{15}P$	$C_{18}Cl_{15}OP{\cdot}C_2Cl_4$	$C_{18}F_2Cl_{15}P{\cdot}C_7H_8$
M_t [g mol^{-1}]	778.90	960.72	909.03
T [K]	100(1)	100(1)	100(1)
λ [pm]	71.073	71.073	71.073
crystal system	triclinic	triclinic	orthorhombic
space group	$P\bar{1}$	$P\bar{1}$	$Pccn$
a [pm]	867.07(2)	943.88(1)	840.13(2)
b [pm]	919.24(2)	1313.83(2)	1532.27(5)
c [pm]	1728.61(4)	1395.72(8)	2469.44(7)
α [°]	100.631(2)	113.281(1)	90
β [°]	100.812(2)	101.7670(1)	90
γ [°]	98.546(2)	96.317(1)	90
V [nm^3]	1.30593(6)	1.53380(4)	3.1789 (2)
Z	2	2	4
ρ [g cm^{-3}]	1.981	2.080	1.899
μ [mm^{-1}]	1.652	1.767	1.381
$F(000)$	756	932	1784
2θ range [°]	4.4–32.2	4.2–28.9	4.2–28.8
no. of reflns collected	12987	33823	15145
no. of unique reflns	8050	7309	3771
R(int)	0.0261	0.0347	0.0597
final R indices [$I > 2\theta(I)$][a]			
R_1	0.0453	0.0387	0.0403
wR_2	0.1002	0.1055	0.0664
R indices (all data)			
R_1	0.0693	0.0536	0.0787
wR_2	0.1151	0.1096	0.0716
Goodness-of-fit[b] on F^2	1.038	1.090	1.025
CCDC RefCode	2359657	2359658	2359659

[a] $R_1 = \sum(|F_o| - |F_c|) / \sum|F_o|$; $wR_2 = [\sum w(F_o^2 - F_c^2)^2 / \sum w(F_o^2)^2]^{1/2}$.
[b] Goodness-of-fit = $[\sum w(F_o^2 - F_c^2)^2 / (n_{obs} - n_{param})]^{1/2}$.

4.6. Computational details

Quantum mechanical calculations have been performed with the Gaussian16 package [72], at the DFT/M06 level of theory with an ultrafine grid option [73] and supplemented with Grimme's dispersion correction D3 [74]. H, C, O, F and Cl atoms have been described using 6–31+g* basis sets [75], whereas P and Ni atoms have been described using Def2-SVPD basis sets [76]. The potential energy surfaces of the studied complexes have been examined at this level of theory, in the gas phase. The geometries of the different complexes have been optimized with no symmetry restrictions. Frequency calculations have been performed in all the collected stationary points in order to check their nature of minima or transition states. Optimized structures of selected perchlorophenyl-derivatives are shown in Fig. S1. $\%V_{bur}$ values for the R_3P phosphines of choice (Table 2) were calculated from the corresponding $R_3P{-}Ni(CO)_3$ complex using the SambVca 2.1 online tool [40]. Atomic coordinates for all the optimized structures are included as a separate *.xyz* file (Appendix B).

CRediT authorship contribution statement

Mª Ángeles García-Monforte: Methodology, Investigation. **Miguel Baya:** Validation, Software, Methodology, Formal analysis. **Antonio Martín:** Validation, Resources, Methodology, Funding acquisition, Formal analysis, Data curation. **Babil Menjón:** Writing – review & editing, Writing – original draft, Supervision, Investigation.

Declaration of competing interest

The authors declare that they have no known competing financial interests or personal relationships that could have appeared to influence the work reported in this paper.

Data availability

Data will be made available on request.

Acknowledgments

This work was supported by the Spanish MCIU/FEDER (Project PID2021–122869NB-I00) and the Gobierno de Aragón (E17_23R). BIFI (Instituto de Biocomputación y Física de Sistemas Complejos) and CESGA (Centro de Supercomputación de Galicia) are acknowledged for allocation of computational resources.

Supplementary materials

Supplementary material associated with this article can be found, in the online version, at doi:10.1016/j.jorganchem.2024.123385.

References

[1] (a) A. Schier, H. Schmidbaur, «P-Donor Ligands», in: R.B. King (Ed.), Encyclopedia of Inorganic Chemistry, 2nd ed., Wiley, Chichester (UK), 2005, pp. 4101–4128;
(b) J.H. Downing, M.B. Smith, «Phosphorus Ligands», in: J.A. McCleverty, T. J. Meyer (Eds.), Comprehensive Coordination Chemistry II, Elsevier, Amsterdam, 2003, pp. 253–296. Vol. 1, Ch. 12;
(c) F.R. Hartley, *Organophosphorus Compounds*, belonging to *Patai's Chemistry of Functional Groups*, Wiley, Chichester (UK), 1990;
(d) C.A. McAuliffe, «Phosphorus, Arsenic, Antimony and Bismuth Ligands», in: G. Wilkinson, R.G. Gillard, J.A. McCleverty (Eds.), Comprehensive Coordination Chemistry, Pergamon Press, Oxford (UK), 1987, pp. 989–1066. Vol. 2, Ch. 14.
[2] A. Michaelis, L. Gleichmann, «Ueber Di- und Triphenylphosphin», Ber. dtsch. chem. Ges. 15 (1882) 801.
[3] J. Svara, N. Weferling, T. Hofmann, «Phosphorus Compounds, Organic». Ullmann's Encyclopedia of Industrial Chemistry, Wiley-VCH, Weinheim (DE), 2006, pp. 19–49.
[4] J. Fernández-Valparís, S. Alvarez, «Design of a structural database for homoleptic transition metal complexes», Struct. Chem. 26 (2015) 1715.
[5] R.T. Boeré, Y. Zhang, «Extremely bulky triarylphosphines incorporating 2,6-diisopropylphenyl substituents; consideration of steric shielding and steric pressure», J. Organomet. Chem. 690 (2005) 2651.
[6] A.N. Sobolev, L.A. Chetkina, I.P. Romm, E.N. Gur'yanova, «Structure of tris(2,6-dimethylphenyl)phosphine», J. Struct. Chem. 17 (1976) 83. *Zh. Strukt. Khim.* 17 (1976) 103.
[7] (a) J.F. Blount, D. Camp, R.D. Hart, P.C. Healy, B.W. Skelton, A.H. White, «The synthesis and structural characterization of mesityldiphenylphosphine, dimesitylphenylphosphine and trimesitylphosphine», Aust. J. Chem. 47 (1994) 1631;
(b) J.F. Blount, C.A. Maryanoff, K. Mislow, «Molecular structure of trimesitylphosphine: An unprecedented enlargement of valence bond angles in a phosphine», Tetrahedron Lett 16 (1975) 913.
[8] R.T. Boeré, A.M. Bond, S. Cronin, N.W. Duffy, P. Hazendonk, J.D. Masuda, K. Pollard, T.L. Roemmele, P. Tran, Y. Zhang, «Photophysical, dynamic and redox behavior of tris(2,6-diisopropylphenyl)phosphine», New J. Chem. 32 (2008) 214.
[9] S. Sasaki, K. Sutoh, F. Murakami, M. Yoshifuji, «Synthesis, structure, and redox properties of the extremely crowded triarylpnictogens: Tris(2,4,6-triisopropylphenyl)phosphine, arsine, stibine, and bismuthine», J. Am. Chem. Soc. 124 (2002) 14830.
[10] S. Sasaki, «Sterically crowded triarylphosphines bearing cyano groups», Tetrahedron Lett. 59 (2018) 2251.
[11] S. Sasaki, K. Sasaki, M. Yoshifuji, «Synthesis, structure, and properties of tris(2,6-diisopropyl-4-methoxyphenyl)phosphine», Phosphorus, Sulfur Silicon Relat. Elem. 183 (2008) 410.
[12] K. Sutoh, S. Sasaki, M. Yoshifuji, «Synthesis and redox properties of crowded triarylphosphines possessing ferrocenyl groups», Inorg. Chem. 45 (2006) 992.
[13] (a) M. Wu, M. Li, L. Yuan, F. Pan, «"Useless channels" in a molecular crystal formed via F···F and F···π halogen bonds», Cryst. Growth Des. 22 (2022) 971;
(b) A. Karipides, C.M. Cosio, «Structure of tris(pentafluorophenyl)phosphine», Acta Crystallogr., Sect. C 45 (1989) 1743.
[14] J. Wesemann, P.G. Jones, D. Schomburg, L. Heuer, R. Schmutzler, «Phosphorus derivatives of anthracene and their dimers», Chem. Ber. 125 (1992) 2187.
[15] (a) W.A. Sheppard, «Pentafluorophenyl group. Electronic effect as a substituent», in: J. Am. Chem. Soc., 92, 1970, p. 5419;
(b) R.J. Blagg, T.R. Simmons, G.R. Hatton, J.M. Courtney, E.L. Bennett, E. J. Lawrence, G.G. Wildgoose, «Novel $B(Ar')_2(Ar'')$ hetero-tri(aryl)boranes: A systematic study of Lewis acidity», Dalton Trans. 45 (2016) 6032;
(c) The C_6F_5 and C_6Cl_5 groups were also calculated to exhibit similar proton affinities: I. Hyla-Kryspin, S. Grimme, H.H. Büker, N.M.M. Nibbering, F. Cottet, M. Schlosser, «The gas phase acidity of oligofluorobenzenes and oligochlorobenzenes: About the additivity or non-additivity of substituent effects» Chem. Eur. J. 11 (2005) 1251.
[16] (a) A. Gavezzotti, «Molecular packing and correlations between molecular and crystal properties», in: H.-B. Bürgi, J.D. Dunitz (Eds.), «Molecular packing and correlations between molecular and crystal properties», Structure Correlation (1994) 509–542. Vol. 2;
(b) G.R. Desiraju, J.A.R.P. Sarma, «The chloro–methyl exchange rule and its violations in the packing of organic molecular solids», Proc. Indian Acad. Sci., Chem. Sci. 96 (1986) 599.
[17] M.A. García-Monforte, P.J. Alonso, J. Forniés, B. Menjón, «New advances in homoleptic organotransition-metal compounds: The case of perhalophenyl ligands», Dalton Trans. (2007) 3347.
[18] A.E. Ashley, T.J. Herrington, G.G. Wildgoose, H. Zaher, A.L. Thompson, N.H. Rees, T. Krämer, D. O'Hare, «Separating electrophilicity and Lewis acidity: The synthesis, characterization, and electrochemistry of the electron deficient tris(aryl) boranes $B(C_6F_5)_{3-n}(C_6Cl_5)_n$ ($n = 1–3$)», J. Am. Chem. Soc. 133 (2011) 14727, see, however, Ref. [5].
[19] H. Zhao, J.H. Reibenspies, F.P. Gabbaï, «Lewis acidic behavior of $B(C_6Cl_5)_3$», Dalton Trans. 42 (2013) 608.
[20] S. Postle, V. Podgorny, D.W. Stephan, «Electrophilic phosphonium cations (EPCs) with perchlorinated-aryl substituents: Towards air-stable phosphorus-based Lewis acid catalysts», Dalton Trans. 45 (2016) 14651.
[21] S.S. Dua, R.C. Edmondson, H. Gilman, «Polyhaloaryl compounds containing phosphorus», J. Organomet. Chem. 24 (1970) 703.
[22] J.M. Miller, «Mass spectral studies of some perhalogenoaromatic derivatives», J. Chem. Soc. A (1967) 828.
[23] M.A. García-Monforte, M. Baya, D. Joven-Sancho, I. Ara, A. Martín, B. Menjón, «Increasing Lewis acidity in perchlorophenyl derivatives of antimony», J. Organomet. Chem. 897 (2019) 185.
[24] K.S. Hayes, M. Nagumo, J.F. Blount, K. Mislow, «Structure, optical resolution, and conformational stability of perchlorotriphenylamine», J. Am. Chem. Soc. 102 (1980) 2773.
[25] J. Veciana, J. Carilla, C. Miravitlles, E. Molins, «Free radicals as clathrate hosts: Crystal and molecular structure of 1:1 perchlorotriphenylmethyl radical–benzene», J. Chem. Soc., Chem. Commun. (1987) 812.
[26] A. Otero, P. Royo, «Pentachlorophenyl-arsenic, -antimony and -bismuth compounds», J. Organomet. Chem. 171 (1979) 333.
[27] If applied in this case, the standard extraction of the sparingly soluble neutral phosphine **1** with a non-polar organic solvent would require large volumes and/or high temperatures, as in Ref. [21].
[28] (a) E. Maslowsky Jr., Vibrational Spectra of Organometallics, John Wiley & Sons, Hoboken, NJ, 2019, pp. 591–596. Sect. 27.7;
(b) R. Usón, J. Forniés, «Organopalladium and platinum compounds with pentahalophenyl ligands», Adv. Organomet. Chem. 28 (1988) 219.

[29] J.A. Hermoso, F.H. Cano, M. Martínez-Ripoll, «Distortions of molecular geometry in pentafluorophenyl rings bonded to metals», J. Chem. Crystallogr. 24 (1994) 457.

[30] H. Gildenast, F. Garg, U. Englert, «Sterically crowded tris(2-(trimethylsilyl)phenyl) phosphine —is it still a ligand?», Chem. Eur. J. 28 (2022) e202103555.

[31] (a) H. Kooijman, A.L. Spek, K.J.C. van Bommel, W. Verboom, D.N. Reinhoudt, «A triclinic modification of triphenylphosphine», Acta Crystallogr., Sect. C 54 (1998) 1695;
(b) B.J. Dunne, A.G. Orpen, «Triphenylphosphine: A redetermination», Acta Crystallogr., Sect. C 47 (1991) 345.

[32] C. Palau, Y. Berchadsky, F. Chalier, J.-P. Finet, G. Gronchi, P. Tordo, «Tris (monochlorophenyl)- and tris(dichlorophenyl)phosphines: Molecular geometry, anodic behavior, and ESR studies», J. Phys. Chem. 99 (1995) 158.

[33] (a) W. Grochala, «The generalized maximum hardness principle revisited and applied to atoms and molecules», Phys. Chem. Chem. Phys. 19 (2017) 30964;
(b) R.G. Pearson, «Applying the concepts of density functional theory to simple systems», Int. J. Quantum Chem. 108 (2008) 821.

[34] S. Ikuta, P. Kebarle, M G., T.Chan Bancroft, R.J. Puddephatt, «Basicities of methyl-, methylphenyl-, and phenylphosphines in the gas phase», J. Am. Chem. Soc. 104 (1982) 5899.

[35] (a) G. Ménard, J.A. Hatnean, H.J. Cowley, A.J. Lough, J.M. Rawson, D. W. Stephan, «C–H bond activation by radical ion pairs derived from $R_3P/Al(C_6F_5)_3$ frustrated Lewis pairs and N_2O», J. Am. Chem. Soc. 135 (2013) 6446;
(b) X. Pan, X. Chen, T. Li, Y. Li, X. Wang, «Isolation and X-ray crystal structures of triarylphosphine radical cations», J. Am. Chem. Soc. 135 (2013) 3414.

[36] a) The lone-pair energy of a phosphine can be used as measure of its donor strength: H.M. Senn, D.V. Deubel, P.E. Blöchl, A. Togni, G. Frenking, «Phosphane lone-pair energies as a measure of ligand donor strengths and relation to activation energies» J. Mol. Struct. (TheoChem) 506 (2000) 233;
b) The donor strength of a given phosphine R_3P is also related with the pK_a of its phosphonium conjugate $[R_3PH]^+$: L. Greb, S. Tussing, B. Schirmer, P. Oña-Burgos, K. Kaupmees, M. Lõkov, I. Leito, S. Grimme, J. Paradies, «Electronic effects of triarylphosphines in metal-free hydrogen activation: A kinetic and computational study» Chem. Sci. 4 (2013) 2788.

[37] O. Shyshkov, U. Dieckbreder, T. Drews, A. Kolomeitsev, G.-V. Röschenthaler, K. Seppelt, «The tris(trifluoromethyl)methyl phosphonium ion, $[P(CF_3)_3CH_3]^+$, preparation and structure», Inorg. Chem. 48 (2009) 6083.

[38] (a) D.J. Durand, N. Fey, «Computational ligand descriptors for catalyst design», Chem. Rev. 119 (2019) 6561;
(b) N. Fey, «The contribution of computational studies to organometallic catalysis: descriptors, mechanisms and models», Dalton Trans. 39 (2010) 296.

[39] (a) J. Jover, J. Cirera, «Computational assessment on the Tolman cone angles for P-ligands», Dalton Trans. 48 (2019) 15036;
(b) T.E. Müller, D.M.P. Mingos, «Determination of the Tolman cone angle from crystallographic parameters and a statistical analysis using the crystallographic data base», Transition Met. Chem. 20 (1995) 533;
(c) C.A. Tolman, «Steric effects of phosphorus ligands in organometallic chemistry and homogeneous catalysis», Chem. Rev. 77 (1977) 313.

[40] (a) L. Falivene, Z. Cao, A. Petta, L. Serra, A. Poater, R. Oliva, V. Scarano, L. Cavallo, «Towards the online computer-aided design of catalytic pockets», Nat. Chem. 11 (2019) 872;
(b) H. Clavier, S.P. Nolan, «Percent buried volume for phosphine and *N*-heterocyclic carbene ligands: Steric properties in organometallic chemistry», Chem. Commun. 46 (2010) 841.

[41] L. Zapf, M. Riethmann, S.A. Föhrenbacher, M. Finze, U. Radius, «An easy-to-perform evaluation of steric properties of Lewis acids», Chem. Sci. 14 (2023) 2275.

[42] (a) K.O. Christe, D.A. Dixon, H.P.A. Mercier, J.C.P. Sanders, G.J. Schrobilgen, W. W. Wilson, «Tetrafluorophosphite, $[PF_4]^-$, anion», J. Am. Chem. Soc. 116 (1994) 2850;
(b) K.B. Dillon, A.W.G. Platt, A. Schmidpeter, Z. Zwaschka, W.S. Sheldrick, «Tetrachloro- und Tricyanochlorophosphat(III) Strukturbilder einer auf halbem Wege stehengebliebenen Addition», Z. anorg. allg. Chem. 488 (1982) 7;
(c) K.B. Dillon, T.C. Waddington, «The tetrabromophosphite, PBr_4^- ion», J. Chem. Soc. D (1969) 1317.

[43] O.O. Shyshkov, A.A. Kolomeitsev, B. Hoge, E. Lork, A. Haupt, M. Keßler, G.-V. Röschenthaler, «Synthesis, reactivity and structural properties of trifluoromethylphosphoranides», Chem. Eur. J. 28 (2022) e202104308.

[44] M. Keßler, M. Kapiza, H.-G. Stammler, B. Neumann, G.-V. Röschenthaler, B. Hoge, «Triorganylphosphoranides: Realization of an unusual structural motif utilizing electron withdrawing pentafluoroethyl groups», ChemPlusChem 88 (2023) e202200436.

[45] (a) M. Keßler, L. Hartmann, H.-G. Stammler, B. Neumann, G.-V. Röschenthaler, B. Hoge, «Free difluorobis(pentafluoroethyl)phosphoranide ion and its ligand properties», Inorg. Chem. 61 (2022) 10833;
(b) M. Keßler, H.-G. Stammler, B. Neumann, G.-V. Röschenthaler, B. Hoge, «Difluorobis(pentafluoroethyl)phosphoranide: A promising building block for phosphoranidometal complexes», Inorg. Chem. 60 (2021) 16466.

[46] K.O. Christe, D.A. Dixon, D. McLemore, W.W. Wilson, J.A. Sheehy, J.A. Boatz, «On a quantitative scale for Lewis acidity and recent progress in polynitrogen chemistry», J. Fluorine Chem. 101 (2000) 151.

[47] (a) J. Jover, N. Fey, J.N. Harvey, G.C. Lloyd-Jones, A.G. Orpen, G.J.J. Owen-Smith, P. Murray, D.R.J. Hose, R. Osborne, M. Purdie, «Expansion of the Ligand Knowledge Base for monodentate P-donor ligands (LKB-P)», Organometallics 29 (2010) 6245;
(b) N. Fey, A.C. Tsipis, S.E. Harris, J.N. Harvey, A.G. Orpen, R.A. Mansson, «Development of a Ligand Knowledge Base, Part 1: Computational descriptors for phosphorus donor ligands», Chem. Eur. J. 12 (2006) 291.

[48] L.A. Wall, R.E. Donadio, W.J. Pummer, «Preparation and thermal stability of tetrakis(pentafluorophenyl)silane and tris(pentafluorophenyl)phosphine», J. Am. Chem. Soc. 82 (1960) 4846.

[49] H.G. Ang, W.S. Lien, «Reactions of bis(trifluoromethyl)nitroxyl with tris (pentafluorophenyl)-phosphine, -arsine and -stibine», J. Fluorine Chem. 9 (1977) 73.

[50] See, however: K.C. Eapen, C. Tamborski, «The synthesis of tris-(trifluoromethylphenyl)phosphines and phosphine oxides» J. Fluorine Chem. 15 (1980) 239.

[51] S. Sasaki, K. Sutoh, Y. Shimizu, K. Kato, M. Yoshifuji, «Oxidation of tris(2,4,6-triisopropylphenyl)phosphine and arsine», Tetrahedron Lett. 55 (2014) 322.

[52] (a) P.J. Alonso, I. Ara, A.B. Arauzo, M.A. García-Monforte, B. Menjón, C. Rillo, «σ-Organoniobium compounds with $[NbR_4]^-$ and NbR_4 stoichiometries», Angew. Chem. Int. Ed. 49 (2010) 6143;
(b) J. Forniés, B. Menjón, R.M. Sanz-Carrillo, M. Tomás, N.G. Connelly, J. G. Crossley, A.G. Orpen, «Synthesis and structural characterization of the first isolated homoleptic organoplatinum(IV) compound: $[Pt(C_6Cl_5)_4]$», J. Am. Chem. Soc. 117 (1995) 4295.

[53] K.A. Al-Farhan, «Crystal structure of triphenylphosphine oxide», J. Crystallogr. Spectrosc. Res. 22 (1992) 687.

[54] A.W.G. Platt, K. Singh, «The interactions between the sterically demanding trimesitylphosphine oxide and trimesityphosphine with scandium and selected lanthanide ions», J. Mol. Struct. 1111 (2016) 180.

[55] B.K. Nicholson, S.E. Thwaite, «Tris(pentafluorophenyl)phosphine oxide», Acta Crystallogr., Sect. E 59 (2003) o1700.

[56] E. Bye, W.B. Schweizer, J.D. Dunitz, «Chemical reaction paths. 8. Stereoisomerization path for triphenylphosphine oxide and related molecules: Indirect observation of the structure of the transition state», J. Am. Chem. Soc. 104 (1982) 5893.

[57] M.A. Tius, «Xenon difluoride in synthesis», Tetrahedron 51 (1995) 6605.

[58] K.M. Doxsee, E.M. Hanawalt, T.J.R. Weakley, «Structure of difluorotriphenylphosphorane», Acta Crystallogr., Sect. C 48 (1992) 1288.

[59] J. Grosse, R. Schmutzler, «Phosphorus–fluorine coupling constants and asymmetric phosphorus–fluorine stretching frequencies in difluorophosphoranes, R_3PF_2», Phosphorus Relat. Group V Elem 4 (1974) 49.

[60] D. Bornemann, C.R. Pitts, L. Wettstein, F. Brüning, S. Küng, L. Guan, N. Trapp, H. Grützmacher, A. Togni, «Deoxygenative fluorination of phosphine oxides: A general route to fluorinated organophosphorus(V) compounds and beyond», Angew. Chem. Int. Ed. 59 (2020) 22790.

[61] J.H.W. LaFortune, K.M. Szkop, F.E. Farinha, T.C. Johnstone, S. Postle, D. W. Stephan, «Probing steric influences on electrophilic phosphonium cations: A comparison of $[(3,5\text{-}(CF_3)_2C_6H_3)_3PF]^+$ and $[(C_6F_5)_3PF]^+$», Dalton Trans. 47 (2018) 11411.

[62] R.R. Holmes, J.M. Holmes, R.O. Day, K.C.K. Swamy, V. Chandrasekhar, «Synthesis and molecular structures of fluorophosphoranes, R_3PF_2, isoelectronic with anionic fluorosilicates», Phosphorus, Sulfur Silicon Relat. Elem. 103 (1995) 153.

[63] W.S. Sheldrick, «Tris(pentafluorophenyl)difluorophosphorane», Acta Crystallogr., Sect. B 31 (1975) 1776.

[64] S. Solyntjes, B. Neumann, H.-G. Stammler, N. Ignat'ev, B. Hoge, «Difluorotriorganylphosphoranes for the synthesis of fluorophosphonium and bismuthonium salts», Eur. J. Inorg. Chem. (2016) 3999.

[65] The referred intramolecular *ortho*-Cl···F non-bonded distance (*ca.* 285 pm) is well below the sum of the corresponding van der Waals radii *r*vdW(F) + *r*vdW(Cl) (322 pm in the classical Bondi scale, [66a] and 328 pm in the scale recently deduced by Alvarez). [66b]This comparison, however, is for guidance only: It cannot be overstressed that van der Waals radii apply to the intermolecular realm.

[66] (a) A. Bondi, «van der Waals volumes and radii», J. Phys. Chem. 68 (1964) 441;
(b) S. Alvarez, «A cartography of the van der Waals territories», Dalton Trans. 42 (2013) 8617.

[67] (a) L. Greb, «Lewis superacids: Classifications, candidates, and applications», Chem. Eur. J. 24 (2018) 17881;
(b) L.O. Müller, D. Himmel, J. Stauffer, G. Steinfeld, J. Slattery, G. Santiso-Quiñones, V. Brecht, I. Krossing, «Simple access to the non-oxidizing Lewis superacid $PhF{\longrightarrow}Al(OR^F)_3$ ($R^F = C(CF_3)_3$)», Angew. Chem. Int. Ed. 47 (2008) 7659.

[68] C.B. Caputo, L.J. Hounjet, R. Dobrovetsky, D.W. Stephan, «Lewis acidity of organofluorophosphonium salts: Hydrodefluorination by a saturated acceptor», Science 341 (2013) 1374.

[69] M.D. Rausch, F.E. Tibbetts, H.B. Gordon, «Perhaloaryl-metal chemistry. II. Pentachlorophenyllithium», J. Organomet. Chem. 5 (1966) 493.

[70] CrysAlisRED, CCD camera data reduction program, Rigaku Oxford Diffraction, Oxford, UK, 2019.

[71] G. Sheldrick, «Crystal structure refinement with *SHELXL*», *Acta Crystallogr., Sect. C* 71 (2015) 3.

[72] M.J. Frisch, G.W. Trucks, H.B. Schlegel, G.E. Scuseria, M.A. Robb, J.R. Cheeseman, G. Scalmani, V. Barone, G.A. Petersson, H. Nakatsuji, X. Li, M. Caricato, A. V. Marenich, J. Bloino, B.G. Janesko, R. Gomperts, B. Mennucci, H.P. Hratchian, J. V. Ortiz, A.F. Izmaylov, J.L. Sonnenberg, D. Williams-Young, F. Ding, F. Lipparini, F. Egidi, J. Goings, B. Peng, A. Petrone, T. Henderson, D. Ranasinghe, V. G. Zakrzewski, J. Gao, N. Rega, G. Zheng, W. Liang, M. Hada, M. Ehara, K. Toyota, R. Fukuda, J. Hasegawa, M. Ishida, T. Nakajima, Y. Honda, O. Kitao, H. Nakai, T. Vreven, K. Throssell, J.A. Montgomery Jr., J.E. Peralta, F. Ogliaro, M. J. Bearpark, J.J. Heyd, E.N. Brothers, K.N. Kudin, V.N. Staroverov, T.A. Keith, R. Kobayashi, J. Normand, K. Raghavachari, A.P. Rendell, J.C. Burant, S.S. Iyengar, J. Tomasi, M. Cossi, J.M. Millam, M. Klene, C. Adamo, R. Cammi, J.W. Ochterski, R.L. Martin, K. Morokuma, O. Farkas, J.B. Foresman, D.J. Fox, Gaussian 16, Revision C.01, Gaussian, Inc., Wallingford CT, 2019.

[73] Y. Zhao, D.G. Truhlar, «The M06 suite of density functionals for main group thermochemistry, thermochemical kinetics, noncovalent interactions, excited states, and transition elements: Two new functionals and systematic testing of four M06-class functionals and 12 other functionals», Theor. Chem. Acc. 120 (2008) 215.

[74] S. Grimme, J. Antony, S. Ehrlich, H. Krieg, «A consistent and accurate *ab initio* parametrization of density functional dispersion correction (DFT-D) for the 94 elements H–Pu», J. Chem. Phys. 132 (2010) 154104.

[75] (a) M.M. Francl, W.J. Petro, W.J. Hehre, J.S. Binkley, M.S. Gordon, D.J. DeFrees, J.A. Pople, «Self-consistent molecular orbital methods. XXIII. A polarization-type basis set for second-row elements», J. Chem. Phys. 77 (1982) 3654;
(b) T. Clark, J. Chandrasekhar, G.W. Spitznagel, P. von Ragué Schleyer, «Efficient diffuse function-augmented basis sets for anion calculations. III. The 3-21+G basis set for first-row elements, Li–F», J. Comput. Chem. 4 (1983) 294.

[76] (a) D. Rappoport, F. Furche, «Property-optimized Gaussian basis sets for molecular response calculations», J. Chem. Phys. 133 (2010) 134105;
(b) B. Metz, H. Stoll, M. Dolg, «Small-core multiconfiguration-Dirac–Hartree–Fock-adjusted pseudopotentials for post- d main group elements: Application to PbH and PbO», J. Chem. Phys. 113 (2000) 2563.

[77] C.A. Jolly, F. Chan, D.S. Marynick, «Calculated inversion barriers and proton affinities for $P(CH_3)_3$ and $P(C_6H_5)_3$», Chem. Phys. Lett. 174 (1990) 320.

[78] E.P.L. Hunter, S.G. Lias, «Evaluated gas phase basicities and proton affinities of molecules: An update», J. Phys. Chem. Ref. Data 27 (1998) 413.